

Phosphorylation of serines 635 and 645 of human Rad17 is cell cycle regulated and is required for G₁/S checkpoint activation in response to DNA damage

Sean Post*, Yi-Chinn Weng*, Karlene Cimprich†, Lan Bo Chen‡, Yang Xu§, and Eva Y.-H. P. Lee*¶

*Department of Molecular Medicine/Institute of Biotechnology, University of Texas Health Science Center, 15355 Lambda Drive, San Antonio, TX 78245; †Department of Molecular Pharmacology, Stanford University, Palo Alto, CA 94305; ‡Dana-Farber Cancer Institute, Harvard Medical School, Boston, MA 02115; and §Department of Biology, University of California at San Diego, La Jolla, CA 92093

Edited by Eric N. Olson, University of Texas Southwestern Medical Center, Dallas, TX, and approved September 18, 2001 (received for review July 16, 2001)

ATR [ataxia-telangiectasia-mutated (ATM)- and Rad3-related] is a protein kinase required for both DNA damage-induced cell cycle checkpoint responses and the DNA replication checkpoint that prevents mitosis before the completion of DNA synthesis. Although ATM and ATR kinases share many substrates, the different phenotypes of ATM- and ATR-deficient mice indicate that these kinases are not functionally redundant. Here we demonstrate that ATR but not ATM phosphorylates the human Rad17 (hRad17) checkpoint protein on Ser⁶³⁵ and Ser⁶⁴⁵ *in vitro*. In undamaged synchronized human cells, these two sites were phosphorylated in late G₁, S, and G₂/M, but not in early-mid G₁. Treatment of cells with genotoxic stress induced phosphorylation of hRad17 in cells in early-mid G₁. Expression of kinase-inactive ATR resulted in reduced phosphorylation of these residues, but these same serine residues were phosphorylated in ionizing radiation (IR)-treated ATM-deficient human cell lines. IR-induced phosphorylation of hRad17 was also observed in ATM-deficient tissues, but induction of Ser⁶⁴⁵ was not optimal. Expression of a hRad17 mutant, with both serine residues changed to alanine, abolished IR-induced activation of the G₁/S checkpoint in MCF-7 cells. These results suggest ATR and hRad17 are essential components of a DNA damage response pathway in mammalian cells.

Cell cycle checkpoints activated by stalled replication forks and DNA damage protect genomic integrity by preventing damaged DNA from being replicated and passed on to new daughter cells (1–5). In *Schizosaccharomyces pombe* (*Sp*), conserved checkpoint Rad proteins, including Rad1, Rad3, Rad9, Rad17, Rad26, and Hus1, are required for activation of checkpoint signaling pathways in response to stalled replication forks and DNA damage. Inactivation of any one of the checkpoint *rad* genes abolishes phosphorylation and activation of two downstream kinases, *SpChk1* and *SpCds1* (6, 7), resulting in defective activation of checkpoints. Human homologues of all of the *Sp* checkpoint *rad* genes have been identified, except *rad26*.

The *Sprad3*⁺ gene, the *Saccharomyces cerevisiae* (*Sc*) *MEC1* gene, and the human *ATM* (ataxia-telangiectasia-mutated) and *ATR* (ATM- and Rad3-related) genes encode related protein kinases (8, 9). ATR and ATM are involved in the replication and DNA damage-induced checkpoints (10–14). Although ATM has been extensively studied, it has been difficult to ascertain ATR function because ATR-deficient cells and embryos are not viable (15, 16). ATM deficiency results in hypersensitivity to ionizing irradiation (IR) in humans and mice (17, 18). Similarly, ATR-deficient blastocysts have increased sensitivity to IR that correlates with chromosomal fragmentation (15). By using cells overexpressing kinase-inactive ATR (ATR^{Ki}) under the regulation of doxycycline, an elevated cellular sensitivity to DNA damage, a defective cell cycle response, and a significant loss of cell viability were observed (13, 19). Cellular substrates of ATM/ATR include p53 (20–23) and BRCA1 (24, 25), but

substrates unique to either ATM or ATR are largely unknown. By using random mutagenesis to generate arrays of peptide substrates, preferred substrates of these kinases have been reported (26). The identification of ATR-specific substrates may provide insights into the embryonic lethality of ATR-deficient mice.

The human *Rad17* homologue (27–29), *Sprad17*⁺, and *ScRAD24* share significant homology to the five genes encoding the replication factor C (RFC) subunits (30), which form a pentameric clamp-loading complex (CLC) required for loading proliferating cell nuclear antigen (PCNA) onto DNA during DNA replication (31). *ScRad24* has been shown to form a stable complex with the four small RFC subunits (32), suggesting that a DNA damage-specific RFC-like CLC containing *ScRad24* may exist. The putative *ScRad24*-RFC-CLC has been proposed to serve as a sensor of DNA damage or replication blocks (33) and/or a loader of the PCNA-like hRad1·hRad9·hHus1 complex (34–36). We show here that ATR but not ATM phosphorylates human Rad17 (hRad17) *in vitro*. There are two modes of regulation of Rad17 phosphorylation, one cell cycle- and the other DNA damage-dependent. We demonstrate that IR-mediated phosphorylation of hRad17 is required for checkpoint activation in response to DNA damage.

Materials and Methods

Cell Culture, Treatment for DNA Damage Induction, and Transfection. AT-22IJE-T-EBS (ATM-deficient) and AT-22IJE-T-YZ5 (ATM-complemented) cell lines, which were gifts from Y. Shiloh (University of Tel Aviv, Israel), were cultured in DMEM supplemented with 10% FCS and 100 μg/ml hygromycin. Tetracycline-inducible wild-type ATR (ATR^{WT}) and ATR^{Ki} cell lines were cultured in DMEM supplemented with 10% FCS (GIBCO/BRL) and 400 μg/ml G418. All other cell lines were from the American Type Culture Collection. Hydroxyurea was added to cell culture medium at a final concentration of 1 mM for 24 h. Aphidicolin was added to cell culture medium at a final concentration of 5 μg/ml for 20 h. IR was administered by using a ¹³⁷Cs γ-irradiator (Shepherd, San Fernando, CA) at 2.44 Gy/min. UV irradiation was performed by using UV Stratalinker 2400 (Stratagene). Cell extracts were prepared from mock-, IR-, or

This paper was submitted directly (Track II) to the PNAS office.

Abbreviations: *Sp*, *Schizosaccharomyces pombe*; *Sc*, *Saccharomyces cerevisiae*; ATM, ataxia-telangiectasia-mutated; ATR, ATM- and Rad3-related; hRad17, human Rad17; RFC, replication factor C; CLC, clamp loading complex; IR, ionizing radiation; GST, glutathione S-transferase; ATR^{WT}, wild-type ATR; ATR^{Ki}, kinase-inactive ATR; *Mm*, *Mus musculus*; α-HA, anti-hemagglutinin; EGFP, enhanced green fluorescent protein.

¶To whom reprint requests should be addressed. E-mail: lee@uthscsa.edu.

The publication costs of this article were defrayed in part by page charge payment. This article must therefore be hereby marked "advertisement" in accordance with 18 U.S.C. §1734 solely to indicate this fact.

UV-treated cells 1 h after treatment unless otherwise stated. Transfections of human 293 and MCF-7 cells were performed by using Lipofectamine (GIBCO/BRL) and Fugene-6 (Boehringer Mannheim), respectively, according to the manufacturers' protocols.

Antibodies. ATR monoclonal antibodies were generated in mice immunized with glutathione *S*-transferase (GST)-ATR⁷¹⁰⁻¹¹⁰⁰. Mouse anti (α)-ATM (3E8), and α -hRad17 (31E9) monoclonal antibodies have been described previously (29, 37). Mouse α -HA.11 and α -Flag-M2 antibodies were from Babco (Richmond, CA) and Sigma, respectively. Rabbit α -p53-P-Ser¹⁵ antibodies were purchased from Cell Signaling (Beverly, MA). Phosphopeptide antibodies were raised against keyhole limpet hemocyanin-conjugated peptides and were affinity-purified by using a phosphopeptide column after passage of the antiserum through a control non-phosphopeptide column to remove antibodies reacting with the nonphosphorylated antigen peptide and nonspecific antigens.

Immunoprecipitation and Immunoblotting. Cells lysates were prepared in Nonidet P-40 or lysis 250 buffer as described (38). Proteins in the soluble extracts were incubated with the indicated antibodies followed by incubation with protein G Sepharose beads for 2 h. Immunoprecipitates were washed 4 times in cold Nonidet P-40 lysis buffer or lysis 250 buffer and boiled in SDS-sample buffer. Proteins were separated by SDS/8.0% PAGE and transferred to poly(vinylidene difluoride) (Milli-

pore). Membranes were incubated with the indicated antibodies, and proteins were detected by using the enhanced chemiluminescence kit (ECL, Amersham Pharmacia) or the 5-bromo-4-chloro-3-indolyl phosphate/nitroblue tetrazolium (BCIP/NBT) Color Development Substrate (Promega).

Plasmid Construction and Mutagenesis. Substitutions of alanine for serine residues, S180A, S635A, S645A, and S635A/S645A, were generated by using the QuickChange Site-Directed Mutagenesis kit (Stratagene) according to the manufacturer's protocol. hRad17^{Wt} was cloned into pcDNA3.1 (Invitrogen). By using a PCR strategy, an in-frame N-terminal hemagglutinin (HA)-tag was added to pcDNA3.1-hRad17.

Kinase Assays. Endogenous ATR and ATM were immunoprecipitated from HeLa cells mock-treated or exposed to 10 Gy of IR with purified α -ATR (2B5) or α -ATM (3E8) IgGs. Recombinant Flag-ATR^{Wt} and ATR^{Ki} were immunoprecipitated with α -Flag-M2 antibodies. ATR and ATM kinase assays were performed as described (38). Reaction products were separated by SDS/PAGE and analyzed by Coomassie staining and autoradiography.

Collection of Murine Tissues Samples. One-month-old wild-type (*Atm*^{+/+}) and ATM-deficient (*Atm*^{-/-}) mice (18) were treated with 10 Gy of IR. Mice were killed 1 h after treatment, and tissues were collected and frozen in liquid nitrogen. Cell extracts were prepared by grinding frozen tissues before incubation in lysis buffer as described above.

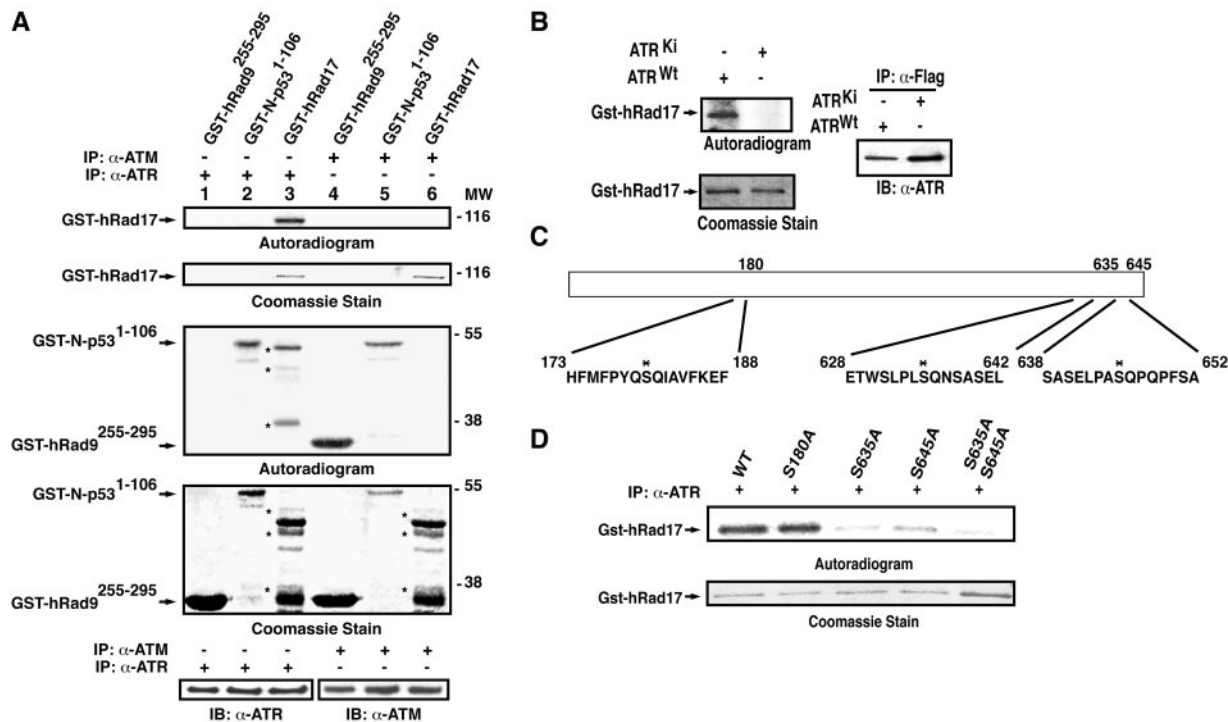


Fig. 1. Phosphorylation of hRad17 on Ser⁶³⁵ and Ser⁶⁴⁵ *in vitro*. (A) Kinase assays using immunoprecipitated (IP) ATM and ATR. GST-hRad17 was incubated with ATM (Top Two Panels, lane 6) and ATR (Top Two Panels, lane 3) immunoprecipitated from HeLa cells treated with 10 Gy of IR. GST-N-p53¹⁻¹⁰⁶, a known substrate of the two kinases, was incubated with ATM (Bottom Two Panels, lane 5) or ATR (Bottom Two Panels, lane 2). GST-hRad9²⁵⁵⁻²⁹⁵, a known substrate of ATM, was incubated with ATM (Bottom Two Panels, lane 4) or ATR (Bottom Two Panels, lane 1). Three micrograms of substrate was used in each reaction. The kinase reaction products were separated by SDS/PAGE and analyzed by Coomassie staining and autoradiography. Levels of ATR and ATM in the kinase reactions were determined by immunoprecipitation followed by Western blotting (IB). MW, molecular weight $\times 10^{-3}$. (B) Kinase assays using recombinant ATR protein. Human kidney 293 cells were transiently transfected with Flag-tagged ATR^{Wt} or ATR^{Ki}. Cells were treated with 10 Gy of IR 36 h after transfection and lysed 1 h after IR. GST-hRad17 fusion proteins were incubated with recombinant ATR immunoprecipitated with α -Flag antibodies. Immunoprecipitation with α -Flag antibodies followed by immunoblotting with α -ATR antibodies confirmed the presence of recombinant ATR. (C) Schematic representation of mutant hRad17 proteins. Site-specific mutation of serine to alanine was confirmed by DNA sequencing. (D) Ser⁶³⁵ and Ser⁶⁴⁵ of hRad17 are substrate sites of ATR *in vitro*. Wild-type and mutant hRad17 fusion proteins were incubated with ATR and the resultant proteins were analyzed as described in B.

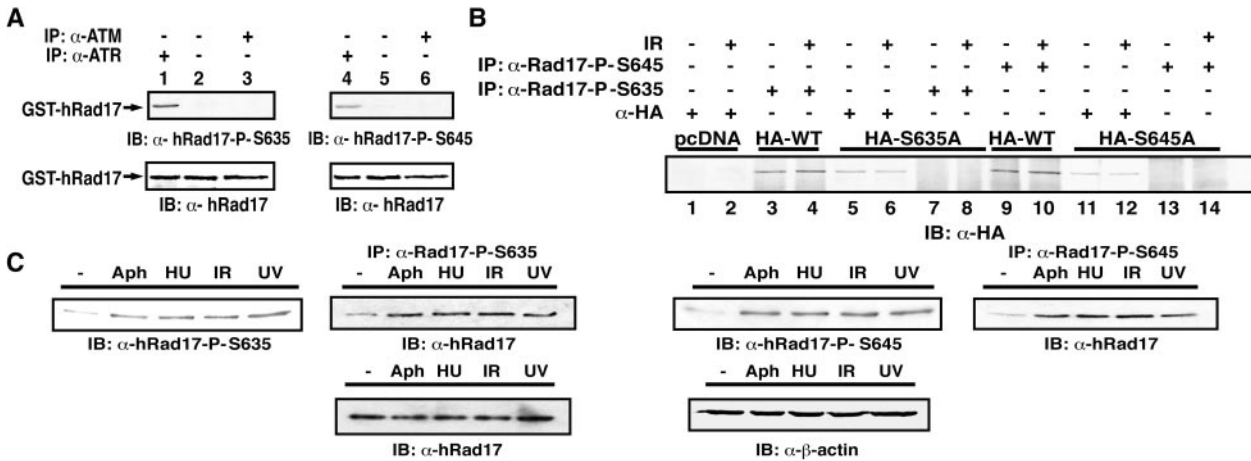


Fig. 2. *In vivo* phosphorylation of hRad17. (A and B) Specificity of the α -hRad17 phosphospecific antibodies. GST-hRad17 was incubated with ATR (A, Top Two Panels, lanes 1 and 4) or ATM (Top Two Panels, lanes 3 and 6), immunoprecipitated from HeLa cells, and immunoblotted with phosphopeptide antibodies. Human kidney 293 cells transfected with HA-tagged hRad17 plasmid as indicated (B). Cells were mock-treated or treated with 10 Gy of IR. Cells were lysed 1 h after treatment, and soluble proteins were immunoprecipitated with α -HA and phosphopeptide antibodies, as indicated. Proteins in the immunoprecipitates were separated by SDS/PAGE and immunoblotted with α -HA antibodies. (C) Phosphorylation of hRad17 on Ser⁶³⁵ and Ser⁶⁴⁵ *in vivo*. Human fibroblast VA-13 cells were mock-treated, treated with 5 μ g/ml aphidicolin (Aph) for 20 h, 1 mM hydroxyurea (HU) for 24 h, 10 Gy of IR, or 50 J/m² UV irradiation. Cells lysates were subjected to SDS/PAGE, and immunoblotting was performed by using the indicated antibodies, or lysates were immunoprecipitated with α -hRad17-P-S635 or α -hRad17-P-S645 antibodies. Immunoblotting of the immunoprecipitated lysates was performed by using α -hRad17 antibody, 31E9. Western blotting analysis of hRad17 protein in the whole cell extracts. Levels of hRad17 and β -actin remain constant in untreated and treated cells.

G₁/S Checkpoint Assay. The G₁/S checkpoint assay was performed by using modifications of a previously described method (39). Briefly, MCF-7 cells cotransfected with pEGFP [which encodes enhanced green fluorescent protein (pEGFP)] and pcDNA3.1, pcDNA3.1-HA-hRad17^{WT}, or pcDNA3.1-HA-hRad17^{S635A/S645A} (10:1 ratio of pcDNA3.1-HA-Rad17 to pEGFP) were exposed to 10 Gy of IR followed by incubation for 24 h at 37°C. Cells were incubated with 10 μ M BrdUrd for 8 h. Immunostaining was performed by using α -BrdUrd antibodies (Becton Dickinson). The percentage of BrdUrd and EGFP double positive cells over EGFP-positive cells was determined for mock- and IR-treated cells, respectively. At least 350 cells were counted from each plate. The mean and SD were calculated from three separate plates.

Results

ATR but Not ATM Phosphorylates Full-Length hRad17 *in Vitro*. To examine whether hRad17 is a substrate of ATR and ATM, *in vitro* kinase assays were performed. Immunoprecipitated ATR, but not ATM, phosphorylated GST full-length hRad17 (Fig. 1A, Upper Two Panels, lanes 3 and 6). The immunoprecipitated ATM was active, as it phosphorylated known substrates, GST-N-p53¹⁻¹⁰⁶ and GST-hRad9²⁵⁵⁻²⁹⁵ (Fig. 1A, Bottom Two Panels, lanes 4 and 5; refs. 23 and 38). ATR also phosphorylated p53 efficiently (23) but did not phosphorylate GST-hRad9²⁵⁵⁻²⁹⁵, an ATM-specific substrate (Fig. 1A, Bottom Two Panels, lanes 1 and 2; ref. 38). The kinase/substrate relationship between ATR and hRad17 was further confirmed by using recombinant wild-type and kinase-inactive ATR (Flag-ATR^{WT} and Flag-ATR^{Ki}), only Flag-ATR^{WT} phosphorylated GST full-length hRad17 (Fig. 1B). These results differentiate ATR and ATM substrate specificity *in vitro* and are in agreement with previous reports that used GST-hRad17 peptides as substrates (26) indicating that residues surrounding the consensus serine and glutamine sites affect phosphorylation of the substrate.

hRad17 Is Phosphorylated on Ser⁶³⁵ and Ser⁶⁴⁵ *in Vitro* and *in Vivo*. Two consensus ATR/ATM phosphorylation sites, Ser⁶³⁵ and Ser⁶⁴⁵, and a nonpreferred serine and glutamine site, Ser¹⁸⁰, are present in hRad17 (Fig. 1C) (26). GST full-length hRad17^{WT} and

GST-hRad17^{S180A} were readily phosphorylated by ATR. On the other hand, substitution of alanine Ser⁶³⁵ and Ser⁶⁴⁵ greatly reduced, but did not abolish, ATR-mediated phosphorylation of hRad17 (Fig. 1D). Taken together, these data demonstrated that GST-hRad17 is phosphorylated mainly on Ser⁶³⁵ and Ser⁶⁴⁵ by ATR *in vitro*, but additional target sites may exist in hRad17.

To determine whether hRad17 is phosphorylated *in vivo*, we first used [³²P]orthophosphoric acid to label cells and demonstrated that hRad17 is a phosphoprotein (data not shown). To confirm indeed Ser⁶³⁵ and Ser⁶⁴⁵ of hRad17 are phosphorylated *in vivo*, phosphospecific antibodies against keyhole limpet hemocyanin-conjugated ETWSLPLS(PO₃)QNSASEL and SASELPAS(PO₃)QPQPFSA peptides were generated, and their specificity was tested by using GST-hRad17. The antibodies react specifically with GST-hRad17 that had been incubated with immunoprecipitated ATR (Fig. 2A, lanes 1 and 4) but not with purified GST-hRad17 or GST-hRad17 incubated with immunoprecipitated ATM (Fig. 2A, lanes 2, 3, 5, and 6). We generated mammalian expression vectors expressing mutant versions of hRad17. Phosphospecific antibodies for Ser⁶³⁵ immunoprecipitated HA-hRad17^{WT} but not HA-hRad17^{S635A} in extracts of transfected, mock- and 10 Gy of IR-treated cells (Fig. 2B, lanes 3, 4, 7, and 8). Similarly, phosphospecific antibodies for Ser⁶⁴⁵ immunoprecipitated HA-hRad17^{WT} but not HA-hRad17^{S645A} in extracts of transfected, mock- and 10 Gy of IR-treated cells (Fig. 2B, lanes 9, 10, 13, and 14). Expression of wild-type and mutant HA-hRad17 was confirmed by immunoprecipitation using α -HA antibodies (Fig. 2B, lanes 5, 6, 11, and 12).

Because ATR activities are up-regulated in response to genotoxic stress (40), we examined whether phosphorylation of both sites of endogenous hRad17 is stimulated by various treatment. There were basal levels of Ser⁶³⁵ and Ser⁶⁴⁵ phosphorylation in untreated asynchronous human fibroblast VA-13 cells, and treating cells with hydroxyurea, a ribonucleotide reductase inhibitor, aphidicolin, a DNA polymerase inhibitor, IR, or UV-irradiation all resulted in elevated phosphorylation of endogenous hRad17 (Fig. 2C). Levels of hRad17 and β -actin remained constant in the untreated or treated cells.

Phosphorylation of hRad17 on Ser⁶³⁵ and Ser⁶⁴⁵ *in Vivo* Is Mediated by ATR. We studied Ser⁶³⁵ and Ser⁶⁴⁵ phosphorylation in cells expressing ATR^{Ki} under regulation of tetracycline (13, 19). On

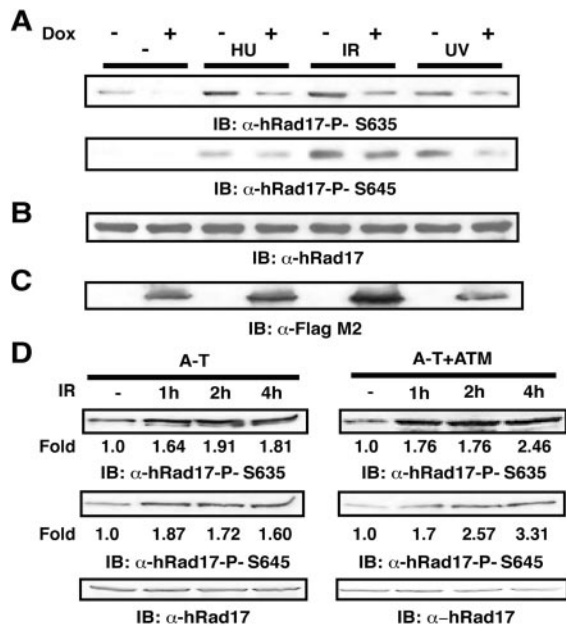


Fig. 3. ATR-dependent phosphorylation of Ser⁶³⁵ and Ser⁶⁴⁵ of hRad17. (A) Analysis of Ser⁶³⁵ and Ser⁶⁴⁵ phosphorylation in cells expressing ATR^{Ki}. Cells expressing ATR^{Ki} under tetracycline regulation were grown in the presence of doxycycline for 72 h. Cells were treated as in Fig. 2C. Soluble proteins were prepared and cell extracts were separated by SDS/PAGE. Immunoblotting was performed by using indicated antibodies. (B) Immunoblotting analysis of hRad17 before and after DNA damage and replication block. Soluble proteins from treated and untreated cells were subjected to SDS/PAGE and immunoblotted with α -hRad17 antibody 31E9. (C) Immunoblotting analysis of recombinant ATR^{Ki} expression. Expression of ATR^{Ki} was determined by SDS/PAGE followed by immunoblotting with α -Flag-M2. (D) ATM-independent phosphorylation of Ser⁶³⁵ and Ser⁶⁴⁵ of hRad17. EBS and YZ5 cells were mock-treated or treated with 30 Gy of IR and harvested 1, 2, or 4 h after treatment. (Bottom) Western blotting analysis of hRad17 in the whole cell extract.

induction of ATR^{Ki}, phosphorylation of Ser⁶³⁵ and Ser⁶⁴⁵ was reduced 2- to 10-fold in untreated cells and cells under genotoxic stress based on densitometric analysis (Fig. 3A and data not shown). Protein levels of hRad17 did not change in response to DNA damage, replication block, or doxycycline treatment (Fig. 3B). Expression of ATR^{Ki} was also similar in untreated and treated cells (Fig. 3C). As reported (25), the residual phosphorylation in cells treated with doxycycline is likely because of the remaining endogenous ATR activities. To test whether ATM is required for phosphorylation of hRad17 Ser⁶³⁵ and Ser⁶⁴⁵ *in vivo*, we analyzed the phosphorylation events by using extracts from EBS (ATM-deficient) and YZ5 (ATM-complemented) cells prepared from mock treatment or 30 Gy of IR at indicated time points (Fig. 3D). Phosphorylation on Ser⁶³⁵ of hRad17 was induced 1.61-, 1.91-, and 1.81-fold in response to DNA damage at 1, 2, and 4 h, respectively, in ATM-deficient cells. Phosphorylation on the same serine in ATM-deficient cells expressing recombinant ATM was induced 1.76-, 1.76-, and 2.46-fold at the same time points. Phosphorylation on Ser⁶⁴⁵ of hRad17 was induced 1.87-, 1.72-, and 1.60-fold in response to DNA damage at 1, 2, and 4 h, respectively, in ATM-deficient cells. Phosphorylation on the same serine in ATM-deficient cells expressing recombinant ATM was induced 1.7-, 2.57-, and 3.31-fold at the same time points. The fold induction in ATM-deficient cells at 4 h after IR is not as apparent, which may be relevant to the higher basal phosphorylation seen in these cells in the absence of DNA damage. These data suggest that ATR, but not ATM, is likely to be the kinase responsible for phosphorylating Ser⁶³⁵

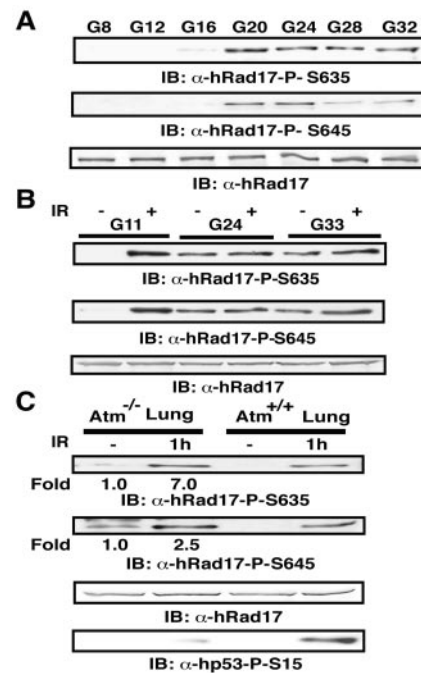


Fig. 4. Cell cycle-dependent phosphorylation of Ser⁶³⁵ and Ser⁶⁴⁵ of hRad17. (A) Immunoblot analysis of phosphorylation at Ser⁶³⁵ and Ser⁶⁴⁵ of hRad17 during the cell cycle. Density-arrested T24 cells were released and harvested at indicated time points G8, G12, G16, G24, G28, and G33 representing 8 h, 12 h, etc. after density release, respectively. Sample analysis was as described in Fig. 2C. (B) Immunoblot analysis of hRad17 phosphorylation during different cell cycle phases. Density-arrested T24 cells were released for 11, 24, and 33 h and harvested 1 h after treatment. (C) Phosphorylation of MmRad17 in mouse tissues. *Atm*^{-/-} and *Atm*^{+/+} mice were mock-treated or treated with 10 Gy of IR and killed 1 h after treatment.

and Ser⁶⁴⁵ of hRad17 in proliferating cells and in cells under genotoxic stress.

Cell Cycle-Dependent Phosphorylation of hRad17. ATM is activated in all cell cycle phases upon DNA damage (9), though our studies using *Xenopus laevis* (*Xl*) extracts have demonstrated that *Xl*ATR plays a role in the S/M checkpoint in the absence of DNA damage (41). Because basal levels of Ser⁶³⁵ and Ser⁶⁴⁵ phosphorylation were detected in asynchronous cell populations without DNA damage (Figs. 2 and 3), we examined whether there is cell cycle-regulated modification of these residues. T24 cells were density-arrested, released, and harvested at specific phases of the cell cycle (42). Ser⁶³⁵ and Ser⁶⁴⁵ became phosphorylated at the start of S phase, and phosphorylation continued throughout the remainder of the cell cycle (Fig. 4A). Protein levels of hRad17 remained constant throughout the cell cycle (Fig. 4A). We next determined whether DNA damage-induced phosphorylation of these residues occurs in a cell cycle-dependent manner. Phosphorylated Ser⁶³⁵ and Ser⁶⁴⁵ were readily detectable in T24 cells in the G₁ phase (G11) on exposure to IR but not in mock-treated cells (Fig. 4B). Similar results were obtained in response to UV treatment (data not shown). In contrast to cells in the G₁ phase, levels of phosphorylation of Ser⁶³⁵ and Ser⁶⁴⁵ were not substantially enhanced during mid-S (G24) and G₂ phases (G33) in response to IR. The cell cycle distribution was confirmed by fluorescence-activated cell sorting analysis, showing $\approx 90\%$ of cells were in G₁ (G11), 60% in S (G24), and 60% in G₂ (G33), respectively, consistent with previous reports (42). To ascertain that the lack of phosphorylation in cells in G₁ phase was not due to prolonged density arrest during cell synchronization, we determined whether *Mus mus-*

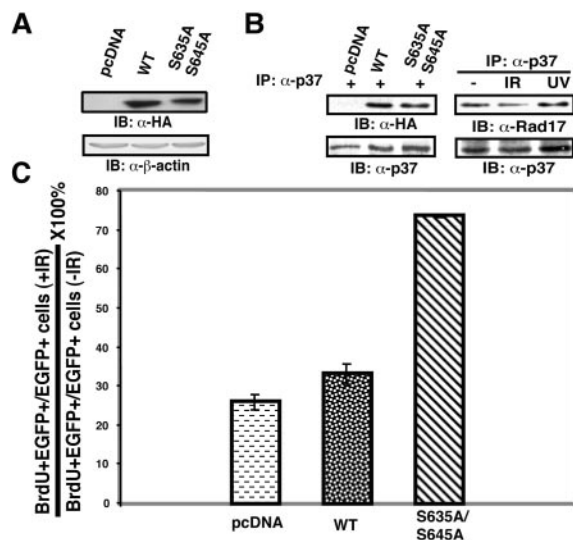


Fig. 5. Effects of expression of hRad17^{S635A} and hRad17^{S645A} on G₁/S checkpoint activation. (A) Immunoblotting analysis of recombinant HA-hRad17 expression in the transfected cells. Proteins in the lysates were separated by SDS/PAGE followed by immunoblotting analysis using α -HA antibody. (B) Recombinant HA-hRad17 and endogenous hRad17 interact with p37/RFC. Immunoprecipitation was carried out by using α -p37/RFC antibodies, and Western blotting was with antibodies as indicated. (C) G₁/S checkpoint activation in response to IR. The ratio of BrdUrd and EGFP double-positive cells to EGFP-positive cells was determined in mock- and IR-treated cells, respectively. At least 350 cells were counted from each plate. The mean and SD were calculated from three separate plates.

culus (Mm)-Rad17 is phosphorylated in terminally differentiated tissues of mice. The two sites, Ser⁶⁴⁷ and Ser⁶⁵⁷, were not phosphorylated in lung and other tissues of the untreated wild-type mice (Fig. 4C and data not shown). Phosphorylation on both sites was readily detected 1 h after IR. Similar to studies using cell lines, levels of total *Mm*Rad17 protein remained constant before and after IR (Fig. 4C). Additionally, there was enhanced phosphorylation on both sites in *Atm*^{-/-} mice in the absence of DNA damage. In *Atm*-deficient mice, there was a 7.0- and 2.5-fold increase in the phosphorylation of *Mm*Rad17 at Ser⁶⁴⁷ and Ser⁶⁵⁷, respectively. In contrast to the *Atm*-deficient mice, no basal phosphorylation was seen in *Mm*Rad17 in wild-type mice, consistent with the observation that hRad17 was not phosphorylated in early and mid G₁ cells. There was a dramatic increase in the phosphorylation of *Mm*Rad17 in wild-type mice; however, because the basal phosphorylation was near zero, the fold increase could not be determined. In contrast to the phosphorylation of *Mm*Rad17, but in agreement with published studies, phosphorylation of Ser¹⁸ of *Mmp53*, the equivalent of Ser¹⁵ human p53 (43), was greatly compromised in the absence of ATM (Fig. 4C; refs. 20–22). Taken together, our data indicate that phosphorylation of Rad17 is enhanced in A-T cells upon IR but the extent of induction may not be optimal, especially at Ser⁶⁴⁵.

Phosphorylation of hRad17 on Ser⁶³⁵ and Ser⁶⁴⁵ Is Required for G₁/S Checkpoint Activation in Response to IR. In subsequent experiments, we determined whether phosphorylation of hRad17 on Ser⁶³⁵ and Ser⁶⁴⁵ is required for G₁/S checkpoint activation. Similar levels of recombinant wild-type and mutant HA-hRad17 were detected in cells transfected with pcDNA3.1-HA-hRad17^{Wt} or pcDNA3.1-HA-hRad17^{S635A/S645A} (Fig. 5A). Both recombinant wild-type and mutant HA-hRad17 interacted with p37/RFC (Fig. 5B). Additionally, unphosphorylated hRad17 from undamaged G₁ synchronized cells and phosphorylated

hRad17 from damaged G₁ synchronized cells interacted with p37/RFC (Fig. 5B), suggesting that phosphorylation of hRad17 is not required for the CLC formation and that the four small RFC subunits form a stable complex as seen in yeast (32). The effects of Ser⁶³⁵ and Ser⁶⁴⁵ phosphorylation on G₁/S checkpoint were assessed by cotransfecting pcDNA3.1, pcDNA3.1-HA-hRad17^{Wt}, or pcDNA3.1-HA-hRad17^{S635A/S645A} and pEGFP at a 10:1 ratio into MCF-7 cells, which express wild-type p53 (44, 45). Overexpression of hRad17^{S635A/S645A} but not vector or wild-type hRad17 (Fig. 5C) abolished IR-induced G₁/S checkpoint activation, suggesting phosphorylation of Ser⁶³⁵ and Ser⁶⁴⁵ of hRad17 is a critical event required for checkpoint activation following DNA damage (Fig. 5C).

Discussion

Our results demonstrate that there are two modes of regulation of phosphorylation on Ser⁶³⁵ and Ser⁶⁴⁵ in hRad17; one is cell cycle-dependent and the other is induced by DNA damage or replication block. We have demonstrated that ATR contributes to both modes of regulation. Additionally, phosphorylation of these two residues of hRad17 is required for IR-induced checkpoint activation.

We have showed that hRad17 is phosphorylated on Ser⁶³⁵ and Ser⁶⁴⁵ in response to DNA damage and replication inhibitors (Fig. 2). Combining data from budding and fission yeast, it appears that hRad17 may be required for cell cycle checkpoint activation in response to genotoxic stress. In addition to the hyperphosphorylation seen in response to DNA damage, phosphorylation of Ser⁶³⁵ and Ser⁶⁴⁵ occurs in undamaged cycling cells during S and G₂/M (Fig. 4). Although it is not clear how ATR activities regulate the S/M checkpoint (46), in *X. laevis* we have shown that *XlATR* is associated with chromatin only during S phase (41). Depletion of *XlATR* from extracts abrogates the S/M checkpoint in the absence of DNA damage, correlating with inhibition of *XlChk1* phosphorylation (41). It is of interest to test whether chromatin association of ATR controls cell cycle-regulated phosphorylation of hRad17. Studies in yeast have demonstrated that *SpRad17* is required for the activation of Chk1; however, whether hRad17 phosphorylation *per se* is required for the S/M checkpoint has yet to be determined.

Overexpression of hRad17 phosphorylation mutants but not wild-type hRad17 abolishes IR-induced G₁/S checkpoint (Fig. 5). How does hRad17 phosphorylation lead to block of cell cycle progression? Studies in multiple organisms have identified signal cascades involved in genotoxic-induced cell cycle checkpoints (1–5). In mammals, phosphorylation of p53 by ATM and ATR and subsequent up-regulation of p21^{Cip1} lead to G₁ arrest. In addition, phosphorylation cascades involving ATM, ATR, Chk1, Chk2, cyclin-dependent kinases, and Cdc25 phosphatases, as well as their yeast counterparts, have been demonstrated. Whether phosphorylation of hRad17 affects these kinases and phosphatases remains to be tested.

Based on kinase assays performed *in vitro* and studies using cells overexpressing ATR^{Ki}, we conclude that ATR contributes to phosphorylation of Ser⁶³⁵ and Ser⁶⁴⁵ of hRad17 with or without genotoxic stress (Figs. 1 and 3). Despite the apparently dispensable role of ATM in hRad17 phosphorylation, it is plausible that optimal phosphorylation of hRad17 may require both kinases, as the reduction of phosphorylation seen in Ser⁶⁴⁵ in ATR^{Ki} cells was not as significant as Ser⁶³⁵. Studies to date suggest that UV- and hydroxyurea-induced phosphorylation of checkpoint proteins are mediated by ATR, and IR-induced phosphorylation is mediated by ATM (23, 25); however, it remains to be seen whether this is true with the expanding list of ATM/ATR substrates.

We consistently observed elevated basal phosphorylation on Ser⁶³⁵ and Ser⁶⁴⁵ in cycling and terminally differentiated (G₀) ATM-deficient cells (Figs. 3 and 4). There are several plausible

explanations for these observations. First, low levels of DNA damage may occur in ATM-deficient cells, leading to phosphorylation of hRad17 by ATR. If this explanation is true, it would indicate ATM and ATR might work synergistically to respond to and to repair DNA damage, as the kinase activity of ATR alone cannot result in the repair of the intrinsic DNA damage in these cells. However, there is no increase in basal phosphorylation of Mmp53 on Ser¹⁸ despite the fact that ATR has been shown to be responsible for the delayed phosphorylation of p53 in response to IR (23). Second, the loss of ATM may result in aberrant hyper-recombination (47), yielding unresolved recombination intermediates, which in turn stimulate the phosphorylation of hRad17 by ATR. These recombination intermediates may result in the high basal phosphorylation seen in the ATM-deficient cell line (EBS), *Atm*^{-/-} mouse embryonic fibroblasts, and *Atm*^{-/-} tissues. Indeed, recombination intermediates have been shown to activate checkpoints through ScRAD24 (48). Third, ATM may negatively regulate ATR activities during G₀ or G₁ cell cycle phases. In the absence of ATM, deregulated ATR may inappropriately interact with and phosphorylate hRad17.

A possible consequence of IR-induced phosphorylation is the enhancement of interaction among hRad17 and other proteins. We have demonstrated that phosphorylation of Ser⁶³⁵ and Ser⁶⁴⁵ of hRad17 is not required for the interaction with p37, one of the small RFC subunits (Fig. 5), suggesting that hRad17 and the four

small RFC subunits form a stable complex as seen in budding yeast (32). Because Rad17 and Rad9-Rad1-Hus1 have been placed in the same epistasis group in yeast and we have demonstrated that ATM phosphorylation of hRad9 is required for G₁/S checkpoint activation (38), it is likely that IR-induced phosphorylation of hRad9 and hRad17, mediated by ATM and ATR, respectively, are both required for checkpoint activation. Although the proposed proliferating cell nuclear antigen clamp-like activities of the mammalian hRad9-hRad1-hHus1 complex has yet to be demonstrated, hRad9 is a 3' to 5' exonuclease (49), suggesting that this exonuclease complex, likely to be loaded by hRad17-RFC-CLC, may remove DNA lesions. Taken together, these data suggest ATM and ATR may phosphorylate unique substrates but work synergistically to maintain genomic stability.

Note. While this manuscript was in preparation, a study by Bao *et al.* (50) on ATM/ATR and hRad17 was published.

We thank Drs. W.-H. Lee, A. Tomkinson, P. Sung, and K. W. McMahon for critical reading of the manuscript and Drs. W.-H. Lee, A. Tomkinson, and M. Chen for stimulating discussions. We are grateful to Drs. D. Levin, S. Zhao, and S.-C. Lin for technical advice and M.-H. Song for technical assistance. Rabbit α -p37/RFC and mouse α -140/RFC were kind gifts from Drs. J. Hurwitz and B. Stillman, respectively. S.P. is a recipient of a Department of Defense training grant. K.A.C. is supported by American Cancer Society Grant RPG99-241-01CCG. E.Y.-H.P.L. is supported by National Institutes of Health Grant P01CA81020.

- Weinert, T. (1998) *Curr. Opin. Genet. Dev.* **8**, 185–193.
- Longhese, M. P., Foiani, M., Muzi-Falconi, M., Lucchini, G. & Plevani, P. (1998) *EMBO J.* **17**, 5525–5528.
- Dasika, G. K., Lin, S. C., Zhao, S., Sung, P., Tomkinson, A. & Lee, E. Y. (1999) *Oncogene* **18**, 7883–7899.
- Caspari, T. & Carr, A. M. (1999) *Biochimie* **81**, 173–181.
- Zhou, B. & Elledge, S. (2000) *Nature (London)* **408**, 433–439.
- Enoch, T., Carr, A. M. & Nurse, P. (1992) *Genes Dev.* **6**, 2035–2046.
- O'Connell, M. J., Raleigh, J. M., Verkade, H. M. & Nurse, P. (1997) *EMBO J.* **16**, 545–554.
- Zakian, V. A. (1995) *Cell* **82**, 685–687.
- Shiloh, Y. (2001) *Curr. Opin. Genet. Dev.* **11**, 71–77.
- Painter, R. B. & Young, R. B. (1980) *Proc. Natl. Acad. Sci. USA* **77**, 7315–7317.
- Canman, C. E., Wolff, A. C., Chen, C. Y., Fornace, A. J., Jr., & Kastan, M. B. (1994) *Cancer Res.* **54**, 5054–5058.
- Cimprich, K. A., Shin, T. B., Keith, C. T. & Schreiber, S. L. (1996) *Proc. Natl. Acad. Sci. USA* **93**, 2850–2855.
- Cliby, W. A., Roberts, C. J., Cimprich, K. A., Stringer, C. M., Lamb, J. R., Schreiber, S. L. & Friend, S. H. (1998) *EMBO J.* **17**, 159–169.
- Guo, Z. & Dunphy, W. G. (2000) *Mol. Biol. Cell* **11**, 1535–1546.
- Brown, E. J. & Baltimore, D. (2000) *Genes Dev.* **14**, 397–402.
- de Klein, A., Muijtjens, M., van Os, R., Verhoeven, Y., Smit, B., Carr, A. M., Lehmann, A. R. & Hoeijmakers, J. H. (2000) *Curr. Biol.* **10**, 479–482.
- Barlow, C., Hirotsune, S., Paylor, R., Liyanage, R., Eckhaus, M., Collins, F., Shiloh, Y., Crawley, J. N., Ried, T., *et al.* (1996) *Cell* **86**, 159–171.
- Xu, Y., Ashley, T., Brainerd, E. E., Bronson, R. T., Meyn, M. S. & Baltimore, D. (1996) *Genes Dev.* **10**, 2411–2422.
- Wright, J. A., Keegan, K. S., Herendeen, D. R., Bentley, N. J., Carr, A. M., Hoekstra, M. F. & Concannon, P. (1998) *Proc. Natl. Acad. Sci. USA* **95**, 7445–7450.
- Banin, S., Moyal, L., Shieh, S., Taya, Y., Anderson, C. W., Chessa, L., Smorodinsky, N. I., Prives, C., Reiss, Y., Shiloh, Y. & Ziv, Y. (1998) *Science* **281**, 1674–1677.
- Canman, C. E., Lim, D. S., Cimprich, K. A., Taya, Y., Tamai, K., Sakaguchi, K., Appella, E., Kastan, M. B. & Siliciano, J. D. (1998) *Science* **281**, 1677–1679.
- Khanna, K. K., Keating, K. E., Kozlov, S., Scott, S., Gatei, M., Hobson, K., Taya, Y., Gabrielli, B., Chan, D., Lees-Miller, S. P., *et al.* (1998) *Nat. Genet.* **20**, 398–400.
- Tibbetts, R. S., Brumbaugh, K. M., Williams, J. M., Sarkaria, J. N., Cliby, W. A., Shieh, S. Y., Taya, Y., Prives, C. & Abraham, R. T. (1999) *Genes Dev.* **13**, 152–157.
- Cortez, D., Wang, Y., Qin, J. & Elledge, S. J. (1999) *Science* **286**, 1162–1166.
- Tibbetts, R., Cortez, D., Brumbaugh, K., Scully, R., Livingston, D., Elledge, S. & Abraham, R. (2000) *Genes Dev.* **14**, 2989–3002.
- Kim, S. T., Lim, D. S., Canman, C. E. & Kastan, M. B. (1999) *J. Biol. Chem.* **274**, 37538–37543.
- Bluyssen, H. A., Naus, N. C., van Os, R. I., Jaspers, I., Hoeijmakers, J. H. & de Klein, A. (1999) *Genomics* **55**, 219–228.
- Dean, F. B., Lian, L. & O'Donnell, M. (1998) *Genomics* **54**, 424–436.
- Bao, S., Chang, M. S., Auclair, D., Sun, Y., Wang, Y., Wong, W. K., Zhang, J., Liu, Y., Qian, X., Sutherland, R., *et al.* (1999) *Cancer Res.* **59**, 2023–2028.
- Griffiths, D. J., Barbet, N. C., McCready, S., Lehmann, A. R. & Carr, A. M. (1995) *EMBO J.* **14**, 5812–5823.
- Podust, V. N., Tiwari, N., Stephan, S. & Fanning, E. (1998) *J. Biol. Chem.* **273**, 31992–31999.
- Green, C. M., Erdjument-Bromage, H., Tempst, P. & Lowndes, N. F. (2000) *Curr. Biol.* **10**, 39–42.
- Griffiths, D., Uchiyama, M., Nurse, P. & Wang, T. S. (2000) *J. Cell Sci.* **113**, 1075–1088.
- Rauen, M., Burtelow, M., Dufault, V. & Karnitz, L. (2000) *J. Biol. Chem.* **275**, 29767–29771.
- Venclovas, C. & Thelen, M. P. (2000) *Nucleic Acids Res.* **28**, 2481–2493.
- Burtelow, M., Roos-Mattjus, P., Rauen, M., Babendure, J. & Karnitz, L. (2001) *J. Biol. Chem.* **276**, 25903–25909.
- Chen, G. & Lee, E. (1996) *J. Biol. Chem.* **271**, 33693–33697.
- Chen, M., Lin, Y., Lieberman, H., Chen, G. & Lee, E. (2001) *J. Biol. Chem.* **276**, 16580–16586.
- Harrington, E. A., Bruce, J. L., Harlow, E. & Dyson, N. (1998) *Proc. Natl. Acad. Sci. USA* **95**, 11945–11950.
- Liu, Q., Guntuku, S., Cui, X. S., Matsuoka, S., Cortez, D., Tamai, K., Luo, G., Carattini-Rivera, S., DeMayo, F., Bradley, A., *et al.* (2000) *Genes Dev.* **14**, 1448–1459.
- Hekmat-Nejad, M., You, Z., Yee, M., Newport, J. & Cimprich, K. (2000) *Curr. Biol.* **10**, 1565–1573.
- Chen, P. L., Scully, P., Shew, J. Y., Wang, J. Y. & Lee, W. H. (1989) *Cell* **58**, 1193–1198.
- Chao, C., Saito, S., Anderson, C. W., Appella, E. & Xu, Y. (2000) *Proc. Natl. Acad. Sci. USA* **97**, 11936–11941. (First Published October 17, 2000; 10.1073/pnas.2202522)
- Gupta, M., Fan, S., Zhan, Q., Kohn, K., O'Connor, P. & Pommier, Y. (1997) *Clin. Cancer Res.* **3**, 1653–1660.
- Fan, S., Smith, M., Rivet, D., Duba, D., Zhan, Q., Kohn, K., Fornace, A. & O'Connor, P. (1995) *Cancer Res.* **55**, 1649–1654.
- Nghiem, P., Park, P. K., Kim, Y., Vaziri, C. & Schreiber, S. L. (2001) *Proc. Natl. Acad. Sci. USA* **98**, 9092–9097.
- Meyn, M. S., Lu-Kuo, J. M. & Herzing, L. B. (1993) *Am. J. Hum. Gen.* **53**, 1206–1216.
- Klein, H. (2001) *Genetics* **157**, 557–565.
- Bessho, T. & Sancar, A. (2000) *J. Biol. Chem.* **275**, 7451–7454.
- Bao, S., Tibbetts, R. S., Brumbaugh, K. M., Fang, Y., Richardson, D. A., Ali, A., Chen, S. M., Abraham, R. T. & Wang, X. F. (2001) *Nature (London)* **411**, 969–974.